

A new route to enhance the ferromagnetic transition temperature in diluted magnetic semiconductors

Kalpataru Pradhan¹, Subrat K Das²

¹*CMP Division, Saha Institute of Nuclear Physics, HBNI, Kolkata 700064, India*

²*SKCG Autonomous College, Paralakhemundi, Odisha 761200, India*

We investigate the magnetic and the transport properties of diluted magnetic semiconductors using a spin-fermion Monte-Carlo method on a 3D lattice in the intermediate coupling regime. The ferromagnetic transition temperature T_c shows an optimization behavior, first increases and then decreases, with respect to the absolute carrier density p_{abs} for a given magnetic impurity concentration x , as seen in the experiment. Our calculations also show an insulator-metal-insulator transition across the optimum p_{abs} where the T_c is maximum. Remarkably, the optimum p_{abs} values lie in a narrow range around 0.11 for all x values and the ferromagnetic T_c increases with x . We explain our results using the polaron percolation mechanism and outline a new route to enhance the ferromagnetic transition temperature in experiments.

Diluted magnetic semiconductors (DMSs) are materials of strong interest due to both, their novel ferromagnetism and potentiality for future spintronics¹⁻⁵. In particular, $\text{Ga}_{1-x}\text{Mn}_x\text{As}$ ^{6,7} with ferromagnetic transition temperature $T_c \simeq 173$ K in bulk⁸, $\simeq 191$ K in films⁹, and even more ($\simeq 200$ K)¹⁰ in nano wires has led intensive efforts to increase T_c in view of possible technological applications.

It is widely accepted that Mn^{2+} ion (Mn_{Ga}) replace Ga^{3+} ion in $\text{Ga}_{1-x}\text{Mn}_x\text{As}$ and thereby contributes a hole to the semiconductor valence band, which mediate the magnetic interaction between the localized spins. However, point defects like Mn interstitials (Mn_I) and As anti-sites^{11,12} significantly compensates the free hole density. In addition, Mn_I are highly mobile and preferentially choose the interstitial positions adjacent to Ga substituted Mn ions (Mn_{Ga}), thus forming anti-ferromagnetic Mn_{Ga} - Mn_I pairs¹³ and consequently increases the Mn inactive sites. So overall Mn_I reduces the hole density and the effective Mn concentration (x_{eff}) to $\text{Mn}_{Ga}-2\text{Mn}_I$ and $\text{Mn}_{Ga}-\text{Mn}_I$, respectively, hindering the higher ferromagnetic T_c in DMSs. We define the carrier density $p = p_{abs}/x$, where x is the Mn concentration and p_{abs} is the absolute carrier density. The p_{abs} in our language is similar to the hole density (holes per cm^3), generally reported in the experiments.

Most of the experimental studies have been devoted in search of room-temperature ferromagnetism using different methods. Post-growth annealing is one of the most extensively used technique which enhances the T_c by reducing the Mn_I concentration and in turn increasing the carrier concentration¹⁴. It is important to note that all Mn_I can not be removed from the sample¹⁵. Even after annealing the fraction of Mn_I increases beyond 0.2 for $x \sim 0.1$, putting a limit to the T_c which either saturates or decreases at larger x ^{16,17}. Consequently, the system goes from insulating to metallic and then again to insulating phase with x ¹⁸.

Another route to enhance the T_c is by p-type and n-type co-doping method that can tune the hole density. It is shown that with Be co-doping both p and

T_c increase for low x ($=0.03$), where as for $x \gtrsim 0.05$ p saturates and T_c decreases due to the increase in Mn_I concentration^{19,20}. In contrast, in Si co-doped samples T_c systematically increases with x even for $x \gtrsim 0.07$ [Ref. 21,22]. It is found that p has lower values in the Si co-doped samples for all values of x . For low x (≤ 0.08) samples the T_c is lower compared to the un-codoped ones^{21,23} and for higher x the co-doped sample shows higher T_c . This enhancement in T_c is attributed to the increase in the hole mobility in the impurity band. In addition, for lower x (≤ 0.08) and higher Si co-doped samples both p and T_c increase as Si start to replace Mn_I sites.

It is believed that it is necessary to increase Mn concentration to enhance the T_c ⁸, but T_c decreases beyond $x_{eff}=0.07$ [Ref. 17]. So it is important to search a route in which both the Mn concentration and the hole density can be altered using growth and post-growth technique. In this letter, we investigate this scenario and outline a procedure to enhance T_c with x . We calculate the ferromagnetic transition temperature within a diluted Kondo lattice model in the intermediate coupling regime using a Monte-Carlo technique based on travelling cluster approximation²⁴ on large size systems. The ferromagnetic T_c shows an optimization behavior with x and p_{abs} , and in the process system undergoes an insulator-metal-insulator transition. Our results qualitatively agree with the recent experiments. We find that optimum p_{abs} , where T_c is maximum, lies around 0.11 for a wide range of $x=0.1-0.35$. For a fixed p_{abs} ferromagnetic T_c increases with x , which suggests a new pathway to achieve high temperature DMSs.

We consider a particle-hole symmetric diluted Kondo lattice Hamiltonian²⁵⁻²⁷ in 3D. The model is given by

$$H = - \sum_{\langle ij \rangle \sigma} t_{ij} c_{i\sigma}^\dagger c_{j\sigma} - \frac{J}{2} \sum_k \mathbf{S}_k \cdot \vec{\sigma}_k - \mu \sum_i n_i,$$

where t is the nearest neighbor hopping parameter, μ is the chemical potential, and J (> 0) is the Hund's coupling between the localized impurity spins \mathbf{S}_k and the itinerant electrons ($\vec{\sigma}_k$) at random impurity sites k .

We assume that the \mathbf{S}_k to be classical unit vectors. We have considered simple cubic lattice with one atom per unit cell, where as GaAs is face centered cubic with four atoms per unit cell. So, roughly 25% of x in our case corresponds to 6.25% that in real experiments. Magnetic moment clustering and hence the direct exchange interaction between the spins are neglected.

In random systems like DMSs the theoretical calculations must adequate a larger system size and also able to capture the effects of spatial fluctuations for a better estimation of any physical quantity such as T_c . Spin-fermion Monte-Carlo is an effective approach to take spatial fluctuations into account^{25,28}. An exact diagonalization scheme is applied to the itinerant carriers in the background of randomly located classical spins \mathbf{S}_k . In order to avoid size limitation we employ a Monte-Carlo technique based on travelling cluster approximation^{24,28} to handle system size as large as $N = L^3 = 10^3$. All physical quantities are averaged over ten different such random configurations. In our particle-hole symmetric model the magnetic and transport properties are presented in terms of the hole density. We set $t = 1$ and all other parameters like J , temperature T are scaled with t .

Magnetic properties in DMSs are consequence of the competition between the carrier mediated ferromagnetic spin-spin interaction and the carrier localization. We start our calculation with a specific choice of $x = 0.25$ and $p = 0.5$ which is a good starting point for simple cubic lattice. For $J \sim 0$ there is no Mn-Mn interaction and for very large J the carriers are trapped in Mn sites. So ferromagnetism is suppressed in these two extreme limits and the optimal T_c lies in the intermediate range of J as shown in Fig.1(a). Carrier localization for higher J leads to the developments of an impurity like band in the density of states, $N(\omega) = \langle \frac{1}{N} \sum_{\alpha} \delta(\omega - \epsilon_{\alpha}) \rangle$ at relatively high temperature $T=0.05$, as shown in Fig.1(b). We estimate T_c from the ferromagnetic structure factor $S(\mathbf{0})$, where $S(\mathbf{q}) = \frac{1}{N} \sum_{ij} \mathbf{S}_i \cdot \mathbf{S}_j e^{i\mathbf{q} \cdot (\mathbf{r}_i - \mathbf{r}_j)}$. The ferromagnetic structure factor for $J=5$, $x=0.25$, and $p=0.5$ is plotted in Fig.1(c) and the inset shows that $S(\mathbf{0})$ for $L=8$ and $L=10$ are barely distinguishable at T_c . So we have considered $L=8$ for rest of our calculations.

We obtain the resistivity for different J values by calculating the dc limit of the conductivity as determined by the Kubo-Greenwood formula^{29,30} as shown in Fig.1(d). At low temperature the system shows metallic behavior for small and intermediate J values. As J increases ($J = 7$) the system remains insulating in the whole temperature range due to carrier localization at impurity sites. Hereafter, we concentrate in the intermediate coupling regime ($J = 5$) where T_c is found to be maximum and relevant to DMSs. Temperature dependence of the resistivity and the ferromagnetic structure factor in Fig.1(c) show one-to-one correspondence between the onset of the ferromagnetism and the metallicity at $T_c = 0.037$.

In carrier-mediated magnetic systems a minimum

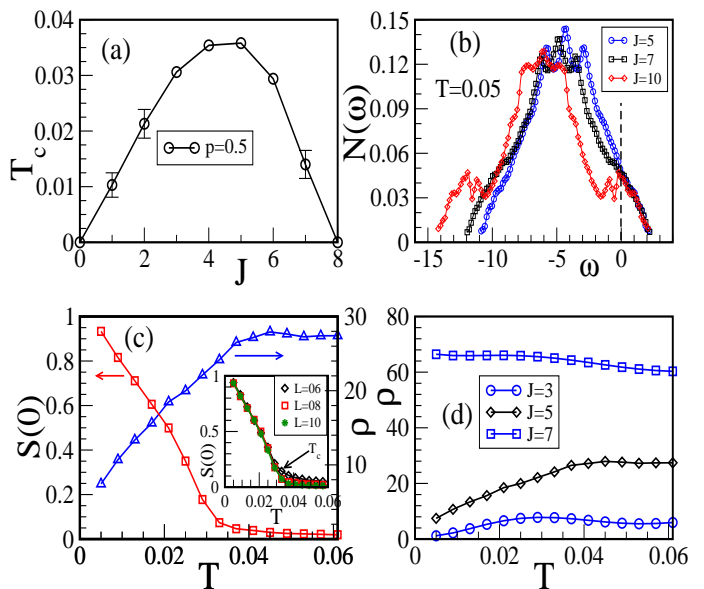


FIG. 1: Color online: (a) ferromagnetic transition temperature T_c for different J values at $p=0.5$; (b) density of states (DOS) at $T=0.05$ for $J=5, 7$, and 10 (Fermi energy is set at zero); (c) temperature dependence of the ferromagnetic structure factor $S(\mathbf{0})$ and resistivity for $J=5$ and $p=0.5$. The inset shows $S(\mathbf{0})$ for three different sizes $L=6, 8$, and 10 . The arrow indicates the T_c ; (d) temperature dependence of the resistivity for $J=3, 5$, and 7 .

amount of carrier is essential to initiate the coupling between the magnetic spins, which depends on J and x . On the other hand, for higher carrier density the magnetism is suppressed due to decrease in carrier mobility. The overall behavior of T_c with p is shown in Fig.2(a) for $J=5$ and $x=0.25$. The mobility picture is confirmed from the conductivity calculation, where T_c and the conductivity (at the low temperature) are maximum at $p=0.45$ (see inset). In order to compare our result with the experiment we plot data from Ref. 17 in Fig. 2(b) such that the impurity concentration x lies in a narrow range from $0.025 - 0.035$ which we assume to be constant. Now if we match, the T_c vs p behavior in the experiment is very similar to our results. A metal-insulator transition with p is also observed in the same experiment (not shown here) which we already illustrated the inset of Fig.2(a).

The carrier mobility and hence the ferromagnetism can be tuned with J , p or x independently. The carrier-spin interaction J is only operative at the impurity sites i.e., for fixed J value the effective coupling strength of the system increases with impurity concentration x . This is similar to the case of increasing J with keeping x fixed. So the variation of T_c with x for fixed p values [Fig. 2(c)] can be understood from the T_c dependence of J as in Fig. 1(a). We plot the experimental data from Ref. 17 in Fig. 2(d) such that the carrier density p lies in a narrow range from $0.86 - 0.93$. We have neglected this small variation of p for qualitative comparison with our calculations and

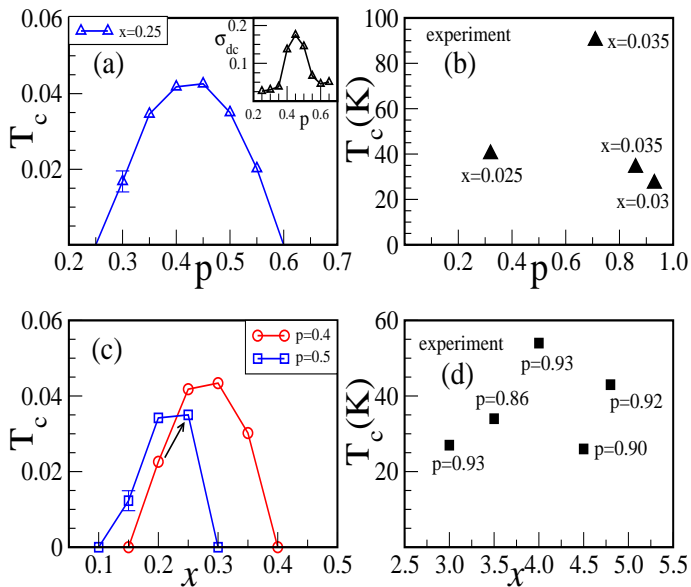


FIG. 2: Color online: For $J=5$ (a) ferromagnetic transition temperature T_c [inset: dc conductivity] for different p values for $x=0.25$ (dc conductivity is calculated at $T=0.005$); (c) Ferromagnetic transition temperature T_c for different x values for $p=0.4$ and 0.5 ; (b) and (d) ferromagnetic transition temperatures T_c taken from the experiment [Ref. 17]. For details please see the text.

found that the T_c shows an optimization behavior with x , quite similar to our results. It is important to note that if we increase both x and p along the arrow shown in Fig. 2(c) the T_c increases, which mimics the effect of post-growth annealing on T_c .

Fig.3(a) shows the ferromagnetic windows for various values of x in a wide range starting from as small as 10%. We find that the optimal p value where the T_c is maximum decreases with x , which is in contrast to the earlier claim where $p=0.5$ is suggested to be the optimum value irrespective of x values²⁵. In experiment, both x and p can be changed simultaneously by co-doping method. It is found that p decreases in the Si co-doped samples for all values of x . Consequently, for low x (≤ 0.08) the T_c decreases as compared to the un-codoped ones^{21,23} and for higher x the co-doped sample has larger T_c . To compare our results with the experiment we focus around $p = 0.4$ in Fig.3(a) (the dotted line). Now, if we decrease p the transition temperature decreases for lower values of x ($=0.25$ and 0.20) but increases for higher values like $x = 0.30$ and 0.35 , which captures the experimental results discussed above. Our calculations clearly demonstrate that the T_c can be increased with x provided the p value is tuned properly but not arbitrarily. For $t=0.5$ eV the estimated T_c is 120 K for $x=0.1$ which qualitatively matches with the experimentally observed T_c range¹⁸.

It is generally believed that the p value must be maximized to obtain a higher ferromagnetic T_c in DMSs. In

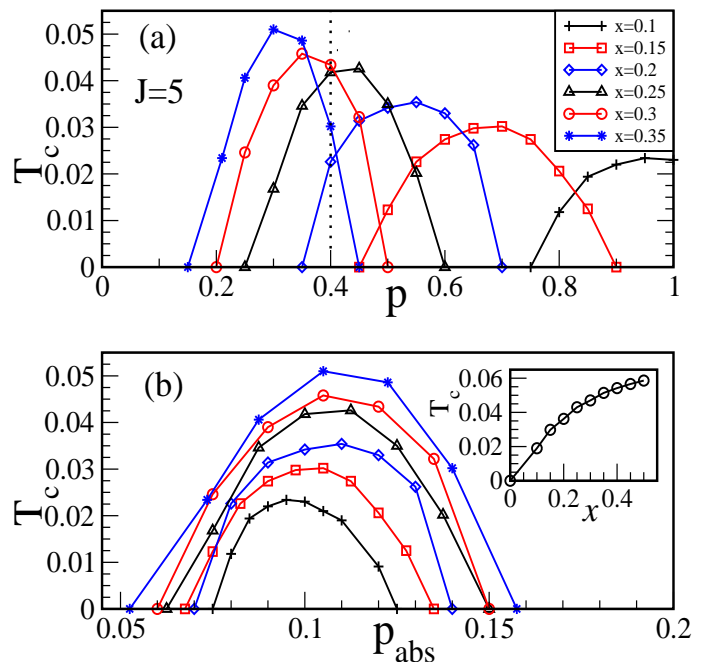


FIG. 3: Color online: Ferromagnetic windows for different magnetic impurity concentrations x . (a) ferromagnetic windows in p and (b) ferromagnetic windows in absolute carrier density, p_{abs} . Inset: variation of transition temperature with x for fixed absolute carrier density, $p_{abs}=0.11$.

Fig.3(a) our calculations show otherwise, that the optimum p value decreases with increasing x . To interpret our finding, in Fig.3(b), we re-plot the ferromagnetic windows in terms of the absolute carrier density p_{abs} as defined earlier. Interestingly, we find that the ferromagnetic windows lie on top of each other with optimum p_{abs} around 0.11 for $x=0.35$, which decreases slightly for smaller x values. To understand this we start our discussion from the double exchange (large J) limit where carrier spins are aligned in the direction of the core spin. For $x = 1$ (spins at each site) carriers get delocalized and the electronic kinetic energy is minimized for the ferromagnetic ground state in the range $0 < p_{abs} < 1$, where the optimum ferromagnetic T_c is found to be at $p_{abs} = 0.5$ [Ref. 31]. This we call the optimum p_{abs} . The range of ferromagnetic ground state is confined to $0 < p_{abs} < 0.3$ in the intermediate coupling regime and the optimum p_{abs} decreases to ~ 0.15 [Ref. 32]. In the diluted limit ($x=0.1-0.35$) we find [see Fig.3(b)] that the optimum p_{abs} value is ~ 0.11 which is in the right ball park as compared to the $x = 1$ limit. This can be understood within a polaron picture discussed below.

In the double exchange limit for one spin and one carrier problem the carrier remains localized to the core spin. A single site localized polaron is shown schematically as the shaded region in Fig.4(a). In the intermediate coupling regime the carrier localization extends over many lattice sites as shown in Fig.4(b). For a given x a minimum concentration of polarons is required for ferromag-

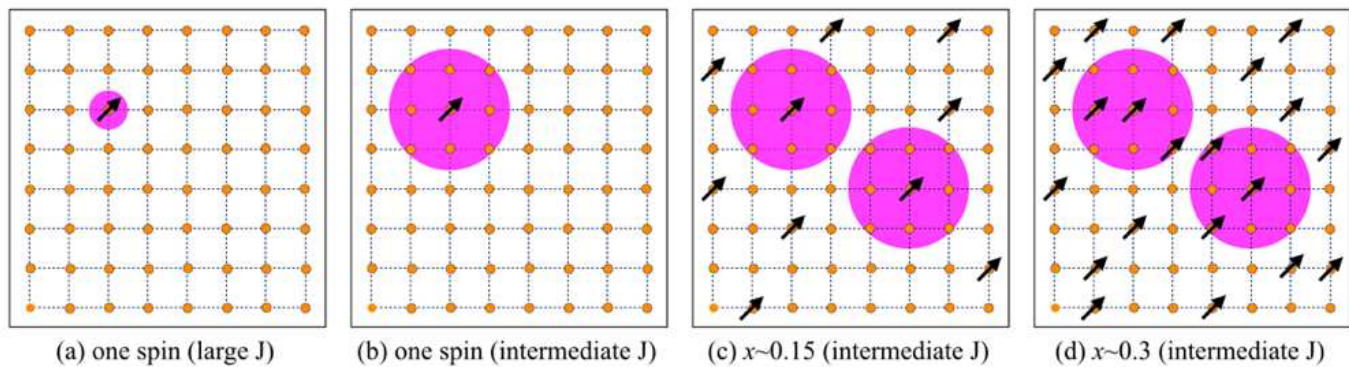


FIG. 4: Color online: Schematic (in 2D) shows the electron delocalization (polarons) by the shaded regions for four different cases; (a) localized polaron in the double exchange limit (large J) and (b) extended polaron in intermediate coupling regime for one spin and one electron case; extended polarons are shown in intermediate coupling regime for two different diluted limits (c) $x = 0.15$ and (d) $x = 0.3$.

netic percolation. For $x=0.15$ the ferromagnetic window starts at $p_{abs} \simeq 0.07$ and T_c is maximum for $p_{abs} \simeq 0.10$. When we increase x the optimum p_{abs} does not change in the range $x=0.1-0.35$, studied in this paper. This indicates that the number of spins in the shaded region increases without affecting the polaron size, schematically shown in Fig.4 (c) and (d). Now if we plot T_c vs x for $p_{abs} = 0.11$, T_c increases with x in the diluted limit and saturates for concentrated x values [see inset of Fig.3(b)].

Using the insight obtained from our calculations we suggest a two step procedure to enhance the ferromagnetic T_c in experiments. The first step is to determine the optimum carrier density p_{abs} for a fixed impurity concentration x . So in this step one needs to tune p_{abs} without changing x , which can be achieved by using an external process like hydrogenation³³. After extracting the optimal p_{abs} the second step is to increase the x only without altering the optimal p_{abs} value obtained in the first step. With increasing x the p_{abs} would change too, which can be tuned back to its optimal value by co-doping with suitable (n-type or p-type) element. It is important to

note that co-doping not only tunes the hole density but also increases the effective x ^{34,35} and will be helpful to enhance the T_c further. We believe that a systematic combination of experimental processes e.g. doping, annealing, hydrogenation, and co-doping can be designed to prepare DMSs with higher T_c .

In conclusion, our model calculations provide a new framework to increase the ferromagnetic T_c in diluted magnetic semiconductors. The optimum p_{abs} (absolute carrier density), where T_c is maximum, lies around 0.11 and T_c increases with x for fixed p_{abs} in a broad range of x studied in this letter. To replicate such a scenario in the experiment, p_{abs} has to be determined for small x and then effort should be made to increase x without altering the p_{abs} value. This procedure, viable in experiments, would enhance the ferromagnetic T_c . We hope that our finding will motivate new experiments by combining the growth and the post-growth process outlined here to achieve high T_c DMSs for spintronics applications.

We acknowledge our discussion with Pinaki Majumdar.

¹ H. Munekata, H. Ohno, S. von Molnar, Armin Segmueller, L. L. Chang, and L. Esaki, Phys. Rev. Lett. **63**, 1849 (1989).

² H. Ohno, Science **281**, 951 (1998).

³ T. Jungwirth, Jairo Sinova, J. Masek, J. Kucera, and A. H. MacDonald, Rev. Mod. Phys. **78**, 809 (2006).

⁴ T. Dietl, Nat. Mat. **9**, 965 (2010).

⁵ T. Dietl and H. Ohno, Rev. Mod. Phys. **86**, 187 (2014).

⁶ H. Ohno, A. Shen, F. Matsukura, A. Oiwa, A. Endo, S. Katsumoto, and Y. Iye, Appl. Phys. Lett. **69**, 363 (1996).

⁷ T. Dietl, H. Ohno, F. Matsukura, J. Cibert, and D. Ferrand, Science **287**, 1019 (2000).

⁸ T. Jungwirth, K. Y. Wang, J. Masek, K. W. Edmonds, Juergen Koenig, Jairo Sinova, M. Polini, N. A. Goncharuk, A. H. MacDonald, M. Sawicki, A. W. Rushforth, R. P.

Campion, L. X. Zhao, C. T. Foxon, and B. L. Gallagher, Phys. Rev. B **72**, 165204 (2005).

⁹ L. Chen, S. Yan, P. F. Xu, J. Lu, W. Z. Wang, J. J. Deng, X. Qian, Y. Ji, and J. H. Zhao, Appl. Phys. Lett. **95**, 182505 (2009).

¹⁰ L. Chen, X. Yang, F. Yang, J. Zhao, J. Misuraca, P. Xiong, and S. von Molnar, Nano Lett. **11**, 2584 (2011).

¹¹ K. M. Yu, W. Walukiewicz, T. Wojtowicz, I. Kuryliszyn, X. Liu, Y. Sasaki, and J. K. Furdyna, Phys. Rev. B **65**, 201303(R) (2002).

¹² R. C. Myers, B. L. Sheu, A. W. Jackson, A. C. Gossard, P. Schiffer, N. Samarth, and D. D. Awschalom, Phys. Rev. B **74**, 155203 (2006).

¹³ J. Blinowski and P. Kacman, Phys. Rev. B **67**, 121204R (2003).

- ¹⁴ S. Potashnik, K. C. Ku, S. H. Chun, J. J. Berry, N. Samarth, and P. Schiffer, *Appl. Phys. Lett.* **79**, 1495 (2001).
- ¹⁵ K. W. Edmonds, P. Boguslawski, K. Y. Wang, R. P. Campion, S. N. Novikov, N. R. S. Farley, B. L. Gallagher, C. T. Foxon, M. Sawicki, T. Dietl, M. Buongiorno Nardelli, and J. Bernholc, *Phys. Rev. Lett.* **92**, 037201 (2004).
- ¹⁶ S. J. Potashnik, K. C. Ku, R. Mahendiran, S. H. Chun, R. F. Wang, N. Samarth, and P. Schiffer, *Phys. Rev. B* **66**, 012408 (2002).
- ¹⁷ M. Dobrowolska, K. Tivakornsasithorn, X. Liu, J. K. Furdyna, M. Berciu, K. M. Yu, and W. Walukiewicz, *Nat. Mat.* **11**, 444 (2012).
- ¹⁸ F. Matsukura, H. Ohno, A. Shen, and Y. Sugawara, *Phys. Rev. B* **57**, R2037(R) (1998).
- ¹⁹ S. Lee, S. J. Chung, and I. S. Choi, *J. Appl. Phys.* **93**, 8307 (2003).
- ²⁰ K. M. Yu, W. Walukiewicz, T. Wojtowicz, W. L. Lim, X. Liu, U. Bindley, M. Dobrowolska, and J. K. Furdyna, *Phys. Rev. B* **68**, 041308(R) (2003).
- ²¹ Y. J. Cho, K. M. Yu, X. Liu, W. Walukiewicz, and J. K. Furdyna, *Appl. Phys. Lett.* **93**, 262505 (2008).
- ²² H. C. Kim, S. Khym, S. Lee, X. Liu, and J. K. Furdyna, *J. Appl. Phys.* **107**, 09C303 (2010).
- ²³ W. Z. Wang, J.J. Deng, J. Lu, L. Chen, Y. Ji, and J.H. Zhao, *Physica E* **41**, 84 (2008).
- ²⁴ S. Kumar and P. Majumdar, *Eur. Phys. J. B* **50**, 571 (2006).
- ²⁵ G. Alvarez, M. Mayr, and E. Dagotto, *Phys. Rev. Lett.* **89**, 277202 (2002).
- ²⁶ A. Chattopadhyay, S. Das Sarma, and A. J. Millis, *Phys. Rev. Lett.* **87**, 227202 (2001).
- ²⁷ Mona Berciu and R. N. Bhatt, *Phys. Rev. Lett.* **87**, 107203 (2001).
- ²⁸ K. Pradhan, A. Mukherjee, and P. Majumdar, *Phys. Rev. Lett.* **99**, 147206 (2007).
- ²⁹ G. D. Mahan, *Quantum Many Particle Physics* (Plenum Press, New York, 1990).
- ³⁰ S. Kumar and P. Majumdar, *Eur. Phys. J. B* **46**, 237 (2005).
- ³¹ S. Yunoki, J. Hu, A. L. Malvezzi, A. Moreo, N. Furukawa, and E. Dagotto, *Phys. Rev. Lett.* **80**, 845 (1998).
- ³² K. Pradhan and P. Majumdar, *Euro. Phys. Lett.* **85**, 37007 (2009).
- ³³ L. Thevenard, L. Largeau, O. Mauguin, and A. Lemaitre, *Appl. Phys. Lett.* **87**, 182506 (2005).
- ³⁴ H. Fujii, K. Sato, L. Bergqvist, P. H. Dederichs, and H. Katayama-Yoshida, *Appl. Phys. Express* **4**, 043003 (2011).
- ³⁵ L. Bergqvist, K. Sato, H. Katayama-Yoshida, and P. H. Dederichs *Phys. Rev. B* **83**, 165201 (2011).